Pythagorean Neutrosophic Normal Interval-Valued Weighted Averaging Approach for Sustainable Financial Risk Prediction

Halla Elziber Elsiddeg Elemam[1,*], Abdelgalal O. I. Abaker[2], Elavarasi Gunasekaran[3], Hago E. M. Ali[4], Abdullah S. Alharbi[5], Amer Alsulami[6], Azhari A Elhag[7]

[1]Department of Administrative Sciences, Applied College, Abha, King Khalid University, Saudi Arabia
[2]Department of Administrative Sciences, Applied College, Khamis Mushait, King Khalid University, Saudi Arabia
[3]Department of Computer Applications, Faculty of Science & Humanities, SRM Institute of Science and Technology, Kattankulathur, Chennai, 603203, India
[4]Department of Business Administration, Faculty of Science and Humanity Studies in Al-Sulail, Prince Sattam Bin Abdulaziz University, Al-Kharj 16278, Saudi Arabia
[5]Department of Finance and Banking, College of Business Administration, Imam Abdulrahman bin Faisal University, DAMMAM 32444, Saudi Arabia
[6]Department of Mathematics, Turabah University College, Taif University, P.O. Box 11099, Taif 21944, Saudi Arabia
[7]Department of Mathematics and Statistics, College of Science, Taif University, P. O. Box 11099, Taif, 21944, Saudi Arabia
Emails: halemam@kku.edu.sa; aoadrees@kku.edu.sa; elavarag4@srmist.edu.in; h.elbasheer@psau.edu.sa; Ashalharbi@iau.edu.sa; al.amer@tu.edu.sa; a.alhag@tu.edu.sa

Abstract

Neutrosophic set (NS) is a prevailing logic aimed at facilitating the understanding of inconsistent and indeterminate data; several kinds of complete or incomplete data can be described as interval-valued NS (IVNS). This study presents aggregation operator for IVNSs and prolongs the generalized weighted aggregation (GWA) operations to congruently work with IVNS information. Also, these results are formulated as IVNSs that are represented by indeterminate, truth, and false degrees. The tremendous growth of financial innovation offers a several convenience to people's lives and production and brings many security risks to financial technology. To avoid financial risk, an improved way is to construct an accurate warning mechanism before the financial risk takes place, not to solve this matter after the risk outbreak. Recently, deep learning (DL) has delivered outstanding results in the natural language processing and image recognition areas. Thus, researcher used DL techniques for the financial risk prediction and obtained satisfactory results. This study develops a new Pythagorean Neutrosophic Normal Interval-Valued Weighted Averaging for Financial Risk Prediction (PNNIVWA-FRP) method using sustainable development. The objective of the PNNIVWA-FRP method is to have two dissimilar stages of processes. Initially, financial data are classified by the PNSNIVWA technique. This method is used for its highest proficiency in managing imprecision and uncertainty in financial data, containing incomplete and ambiguous data. Second, the classified parameter is fine-tuned by means of Glowworm Swarm Optimization (GSO) technique. Based on the luminescent communication of glowworms, GSO is proficient at navigating multidimensional, complex search spaces for identifying better solutions. The empirical findings on benchmark dataset demonstrate the effectiveness of the PNNIVWA-FRP method, showcasing significant development in prediction results than classical approaches.

Keywords: Financial Risk Prediction; Neutrosophic Set; Interval Valued Neutrosophic Set; Weighted Aggregation; Glowworm Swarm Optimization

DOI: https://doi.org/10.54216/IJNS.250224
Received: February 23, 2024 Revised: May 12, 2024 Accepted: August 22, 2024

1. Introduction

Owing to the difficulty and ambiguity of neutral objects, and the uncertainty of individual thinking, Zadeh in 1965 presented an extraordinary concept of fuzzy sets (FSs) [1]. Since that time, the FS concept has been effectively utilized in several fields of multi-attribute decision-making [2]. Additionally, the FSs have been developed extensively, including the hesitant FS (HFSs), interval-valued intuitionistic FS (IVIFS), intuitionistic FS (IFSs), interval-valued FS (IVFSs), etc. However FS theory was advanced and expanded, it is still unable to account for all potential ambiguities and a wide range of physical issues [3]. An NS is a set by which every component of the world has indeterminacy, falsity, and truth degrees, that exist in the unusual entity time of] 0-, 1+ [. and this technique signifies a development of the normal interval [0, 1] utilized for IFS.

Financial risk prediction is a significant and extensively researched area in the field of economic analysis and it can assist businesses in identifying early economic dangers and handling the right activities to reduce failures [4]. Several business risk forecasts contain mostly binary classification difficulties, which denote statements that are allocated to one or more sets after data analysis [5]. Credit risk represents the possibility of the bankrupts not paying their debts and the risk forecasting can separate the account as default or normal [6]. Fraud risk is the danger of business loss caused by the prediction of risk and the scam that is used to categorize a data set as fraud or normal. An accurate economic risk prediction method is essential for preventing the risk of finances at an affordable cost. For a high amount of data, manual processing methods are expensive and time-consuming [7]. So, based on deep learning (DL) and machine learning (ML), the researchers of economic security proposed new economic risk-preventing approaches.

The huge and diverse size of corporate economic data changes constantly with time and makes it difficult to analyse complex corporate economic data [8]. Recently, artificial neural networks (ANN) have been employed extensively with the improvement of big data and ML, due to their strong capability to handle nonlinear mapping difficulties. In the ANN method, the economic risk method based on ML could finish the testing and training of high-dimensional economic data to get effectual study outcomes [9]. Significantly, ML algorithms can resolve the issues of timeliness in forecast and also retain the basic relation among past time series and recent economic values, therefore getting more exact economic crisis forecast outcomes [10]. But, still, now, there is no generalized method for predicting effective corporate economic disasters.

This study develops a new Pythagorean Neutrosophic Normal Interval-Valued Weighted Averaging for Financial Risk Prediction (PNNIVWA-FRP) method using sustainable development. The main purpose of the PNNIVWA-FRP algorithm has two different stages of processes. Initially, financial data are classified by the PNSNIVWA technique. Second, the classified parameter is fine-tuned by employing Glowworm Swarm Optimization (GSO) technique. The empirical findings on benchmark dataset demonstrate the effectiveness of the PNNIVWA-FRP method, showcasing significant development in prediction results than classical approaches.

2. Related Works

In [11], a new credit risk prediction structure is presented known as, Feature Selection–Resample Strategy–ML (FS-RS-ML). Additionally, a Recursive Feature Elimination with Cross-Validation (RFECV) method is used for choosing main feature, which affects SMEs' credit risk prediction, and 3 re-sampling methods have been utilized for balancing the sample data. At last, 5 ML methods are approved to organize the low-risk and high-risk SMEs. Lei et al. [12] introduced an AI-based financial-risk-prevention (FRP) method. At first, related economic index data are gathered, and the particular data features are increased by pre-processing; second, the chaotic grasshopper optimizer algorithm (CGOA) is employed to imitate the grasshoppers' behaviours. Next, the SVM executes data processing with smaller features. The risk of Empirical is measured by the regular operation and a hinge loss function is combined to elevate the structure of risk. At last, the slime mould algorithm (SMA) enhances the method to increase the effectiveness of SVM. In [13], an XGBoost scoring card method is advanced. The research shows: first, the combination of the SMOTE methods with the XGBoost techniques displays specific presentation advantages while handling unbalanced datasets; next, the reliable economic data remains focused on important risk factors; third, the XGBoost scoring card method depends on important characteristics effectually improves the accurateness of credit risk evaluation.

In [14], the backpropagation neural network (BPNN) method is used for constructing an active economic risk pre-alarm method. First, on measuring data economic risk is gathered. Later, it is pre-processed and a primary group of random frameworks is employed to generate BPNN structures that are trained by a part of the gathered information. Then, a genetic method is used to improve the BPNN parameters. Zhang [15] presents an economic organization system based on altered random forest (RF). To optimize the generalizability of economic organization approaches, pruning techniques are implemented to avoid overfitting in the research. Synthetic

DOI: https://doi.org/10.54216/IJNS.250224
Received: February 23, 2024 Revised: May 12, 2024 Accepted: August 22, 2024

minority oversampling method is employed to improve the economic organization method and decrease the calculation deviation method using its sampling capability. Simultaneously, the prediction index method is presented to develop the research capability of the economic organization method. Ma et al. [16] built a new hybrid predicting method for enterprise financing risk. Especially, the data pre-processing modulus mostly recognizes the pre-screening financing risk measures and resolves the predicting task produced by unbalanced data; the FS part depends on dual grey wolf optimization (GWO) is aimed to detect optimum financing risk measures; The predicting segment depends on the developed extreme learning machine (ELM) method is defined in this paper to achieve great predicting accuracy.

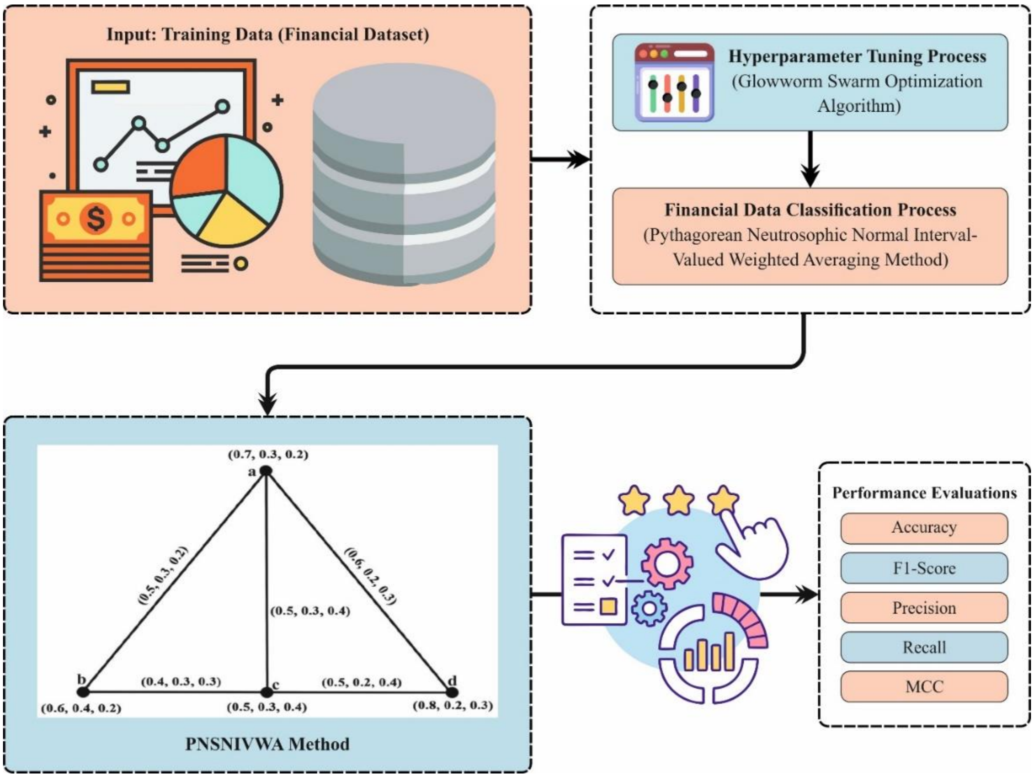

Figure 1. Overall process of PNNIVWA-FRP method

3. The Proposed Method

In this work, we design a novel PNNIVWA-FRP algorithm using sustainable development. The main purposes of the PNNIVWA-FRP algorithm are two different stages of processes are demonstrated in Fig. 1.

A. Stage I: Prediction using PNSNIVWA Classifier

At primary stage, the PNNIVWA-FRP method takes places the classification using PNSNIVWA classifier for financial risk prediction. The basic definition needed for this study is discussed below [17].

Consider $\mathbb{U}$ as a universal dissertation. The PFS Z in $\mathbb{U}$ is $Z = \{u, \langle \zeta_Z^{\mathcal{T}}(u), \zeta_Z^{\mathcal{F}}(u) \rangle | u \in \mathbb{U}\}$, in which the $\zeta_Z^{\mathcal{T}}:\mathbb{U} \rightarrow [0,1]$ and $\zeta_Z^{\mathcal{F}}:U \rightarrow [0,1]$ are the degrees of the component $u \in \mathbb{U}$ to the subset Z, correspondingly, and $0 \leq (\zeta_Z^{\mathcal{T}}(u))^2 + (\zeta_Z^{\mathcal{F}}(u))^2 \leq 1$. $Z = \{\zeta_Z^{\mathcal{T}}, \zeta_Z^{\mathcal{F}}\}$ refers to a Pythagorean fuzzy number (PFN).

Consider $\text{Int}([0,1])$ as the closed subinterval within $[0,1]$. U as universal dissertation. The PIVFS Z in $\mathbb{U}$ is $\hat{Z} = \left\{u, \langle \widehat{\zeta_Z^{\mathcal{T}}}(u), \widehat{\zeta_Z^{\mathcal{F}}}(u) \rangle \middle| u \in \mathbb{U}\right\}$, in which the $\widehat{\zeta_Z^{\mathcal{T}}}:\mathbb{U} \rightarrow Int([0,1])$ and $\widehat{\zeta_Z^{\mathcal{F}}}:\mathbb{U} \rightarrow Int([0,1])$ is the degrees of the component $u \in \mathbb{U}$ to the Z, correspondingly, and $0 \leq (\zeta_Z^{\mathcal{T}+}(u))^2 + (\zeta_Z^{\mathcal{F}+}(u))^2 \leq 1$.

$Z = \langle [\zeta_Z^{\mathcal{T}-}, \zeta_Z^{\mathcal{T}+}], [\zeta_Z^{\mathcal{F}-}, \zeta_Z^{\mathcal{F}+}] \rangle$ Is a PIVFN.

Consider $\mathbb{U}$ as a universal dissertation. The NSS Z in $\mathbb{U}$ is $Z = \{u, \langle \zeta_Z^{\mathcal{T}}(u), \zeta_Z^{\mathcal{I}}(u), \zeta_Z^{\mathcal{F}}(u) \rangle | u \in \mathbb{U}\}$, in which the $\zeta_Z^{\mathcal{T}}: \mathbb{U} \rightarrow [0,1]$, $\zeta_Z^{\mathcal{I}}:\mathbb{U} \rightarrow [0,1]$ and $\zeta_Z^{\mathcal{F}}:\mathbb{U} \rightarrow [0,1]$ are the truth, indeterminacy and false degrees of the component $u \in \mathbb{U}$ to the Z, correspondingly, and $0 \leq \zeta_Z^{\mathcal{T}}(u) + \zeta_Z^{\mathcal{I}}(u) + \zeta_Z^{\mathcal{F}}(u) \leq 3$. $Z = \{\zeta_Z^{\mathcal{T}}, \zeta_Z^{\mathcal{I}}, \zeta_Z^{\mathcal{F}}\}$ is an NSN.

DOI: https://doi.org/10.54216/IJNS.250224
Received: February 23, 2024 Revised: May 12, 2024 Accepted: August 22, 2024

Consider $\mathbb{U}$ as a universal discourse. The PNSS Z in $\mathbb{U}$ is $Z = \{u, \langle \zeta_Z^{\mathcal{T}}(u), \zeta_Z^{\mathcal{I}}(u), \zeta_Z^{\mathcal{F}}(u) \rangle | u \in \mathbb{U}\}$, in which the $\zeta_Z^{\mathcal{T}}: \mathbb{U} \to [0,1]$, $\zeta_Z^{\mathcal{I}}: \mathbb{U} \to [0,1]$, correspondingly, and $0 \le (\zeta_Z^{\mathcal{T}}(u))^2 + (\zeta_Z^{\mathcal{I}}(u))^2 + (\zeta_Z^{\mathcal{F}}(u))^2 \le 2. = \{\zeta_Z^{\mathcal{T}}, \zeta_Z^{\mathcal{I}}, \zeta_Z^{\mathcal{F}}\}$ is a PNSN.

Consider $Z = \langle [\zeta^{\mathcal{T}-}, \zeta^{\mathcal{T}+}], [\zeta^{\mathcal{F}-}, \zeta^{\mathcal{F}+}] \rangle$, $Z_1 = \langle [\zeta_1^{\mathcal{T}-}, \zeta_1^{\mathcal{T}+}], [\zeta_1^{\mathcal{F}-}, \zeta_1^{\mathcal{F}+}] \rangle$ and $Z_2 = \langle [\zeta_2^{\mathcal{T}-}, \zeta_2^{\mathcal{T}+}], [\zeta_2^{\mathcal{F}-}, \zeta_2^{\mathcal{F}+}] \rangle$ as three PIVFNs, and $r > 0$.

1. $Z_1 \oplus Z_2 =$

$$\left[\begin{matrix}\left[\sqrt{(\zeta_1^{\mathcal{T}-})^2 + (\zeta_2^{\mathcal{T}-})^2 - (\zeta_1^{\mathcal{T}-})^2 \cdot (\zeta_2^{\mathcal{T}-})^2}, \sqrt{(\zeta_1^{\mathcal{T}+})^2 + (\zeta_2^{\mathcal{T}+})^2 - (\zeta_1^{\mathcal{T}+})^2 \cdot (\zeta_2^{\mathcal{T}+})^2}\right], \\ [\zeta_1^{\mathcal{F}-} \cdot \zeta_2^{\mathcal{F}-}, \zeta_1^{\mathcal{F}+} \cdot \zeta_2^{\mathcal{F}+}]\end{matrix}\right],$$

2. $Z_1 \otimes Z_2 =$

$$\left[\begin{matrix}[\zeta_1^{\mathcal{T}-} \cdot \zeta_2^{\mathcal{T}-}, \zeta_1^{\mathcal{T}+} \cdot \zeta_2^{\mathcal{T}+}], \\ \left[\sqrt{(\zeta_1^{\mathcal{F}-})^2 + (\zeta_2^{\mathcal{F}-})^2 - (\zeta_1^{\mathcal{F}-})^2 \cdot (\zeta_2^{\mathcal{F}-})^2}, \sqrt{(\zeta_1^{\mathcal{F}+})^2 + (\zeta_2^{\mathcal{F}+})^2 - (\zeta_1^{\mathcal{F}+})^2 \cdot (\zeta_2^{\mathcal{F}+})^2}\right]\end{matrix}\right],$$

3. $r \cdot Z = \left[\left[\sqrt{1-(1-(\zeta^{\mathcal{T}-})^2)^r}, \sqrt{1-(1-(\zeta^{\mathcal{T}+})^2)^r}\right], [(\zeta^{\mathcal{F}-})^r, (\zeta^{\mathcal{F}+})^r]\right]$,

4. $z^r = \left[[(\zeta^{\mathcal{T}-})^r, (\zeta^{\mathcal{T}+})^r], \left[\sqrt{1-(1-(\zeta^{\mathcal{F}-})^2)^r}, \sqrt{1-(1-(\zeta^{\mathcal{F}+})^2)^r}\right]\right]$.

For $Z = \{[\zeta^{\mathcal{T}-}, \zeta^{+}], [\zeta^{\mathcal{F}-}, \zeta^{\mathcal{F}+}$ the score function of Z is given below:

$$S(Z) = \frac{1}{2}((\zeta^{\mathcal{T}-})^2 + (\zeta^{\mathcal{T}+})^2 - (\zeta^{\mathcal{F}-})^2 - (\zeta^{\mathcal{F}+})^2), S(Z) \in [-1,1],$$

and the function of Z is given below:

$$H(Z) = \frac{1}{2}((\zeta^{\mathcal{T}-})^2 + (\zeta^{\mathcal{T}+})^2 + (\zeta^{\mathcal{F}-})^2 + (\zeta^{\mathcal{F}+})^2), H(Z) \in [0,1].$$

Consider R as a real number set, the $M(x) = e^{-(\frac{x-\theta}{\delta})^2}$, $(\delta > 0)$ indicates a normal fuzzy number (NFN) $M = (\theta, \delta)$ and the NFNS is represented as $\widehat{N}$.

Consider $L = (\theta_1, \delta_1) \in \widehat{N}$ and $M = (\theta_2, \delta_2) \in \widehat{N}$, $(\delta_1, \delta_2 > 0)$, then the distance between L and M is $\mathbb{D}(L, M)$ and $(L, M) = \sqrt{(\theta_1 - \theta_2)^2 + \frac{1}{2}(\delta_1 - \delta_2)^2}$, where $\widehat{N}$ is NFNS.

The concept of PNSIVN and NFN its functions are given below.

Assume Int $([0,1])$ as the closed subinterval in [0,1]. $\mathbb{U}$ as a universal dissertation. The PNSIVS $\hat{Z}$ in $\mathbb{U}$ refers to $\hat{Z} = \{u, \langle \widehat{\zeta_Z^{\mathcal{T}}}(u), \widehat{\zeta_Z^{\mathcal{I}}}(u), \widehat{\zeta_Z^{\mathcal{F}}}(u) \rangle | u \in \mathbb{U}\}$, in which the $\widehat{\zeta_Z^{\mathcal{T}}}: \mathbb{U} \to Int([0,1])$, $\widehat{\zeta_Z^{\mathcal{I}}}: \mathbb{U} \to Int([0,1])$ and $\widehat{\zeta_Z^{\mathcal{F}}}: \mathbb{U} \to Int([0,1])$ are the degrees of the component $u \in \mathbb{U}$ to the $\hat{Z}$, correspondingly, and $0 \le (\widehat{\zeta_Z^{\mathcal{T}}}(u))^2 + (\widehat{\zeta_Z^{\mathcal{I}}}(u))^2 + (\zeta_Z^{\mathcal{F}}(u))^2 \le 2$, Note that $0 \le (\zeta_Z^{\mathcal{T}+}(u))^2 + (\zeta_Z^{\mathcal{I}+}(u))^2 + (\zeta_Z^{\mathcal{F}+}(u))^2 \le 2$. $\hat{Z} = \{[\zeta_Z^{\mathcal{T}-}, \zeta_Z^{\mathcal{T}+}], [\zeta_Z^{\mathcal{I}-}, \zeta_Z^{\mathcal{I}+}], [\zeta_Z^{\mathcal{F}-}, \zeta_Z^{\mathcal{F}+}]\}$ is a PNSIVN.

For PNSIVN $\hat{Z} = \langle [\zeta_Z^{\mathcal{T}-}, \zeta_Z^{\mathcal{T}+}], [\zeta_Z^{\mathcal{I}-}, \zeta_Z^{\mathcal{I}+}], [\zeta_Z^{\mathcal{F}-}, \zeta_Z^{\mathcal{F}+}] \rangle$, the score function of $\hat{Z}$ is:

$$S(\hat{Z}) = \frac{\theta}{2}\left(\frac{(\zeta^{\mathcal{T}-})^2 + (\zeta^{\mathcal{T}+})^2}{2} - \frac{(\zeta^{\mathcal{I}-})^2 + (\zeta^{\mathcal{I}+})^2}{2} + 2 - \frac{(\zeta^{\mathcal{F}-})^2 + (\zeta^{\mathcal{F}+})^2}{2}\right), S(\hat{Z}) \in [-1,1].$$

Consider $(\theta, \delta) \in \widehat{N}$, $\hat{Z} = \langle (\theta, \delta); [\zeta^{\mathcal{T}-}, \zeta^{\mathcal{T}+}], [\zeta^{\mathcal{I}-}, \zeta^{\mathcal{I}+}], [\zeta^{\mathcal{F}-}, \zeta^{\mathcal{F}+}] \rangle$as a PNSNIVN, the truth, indeterminacy and falsity degrees are $[\zeta^{\mathcal{T}-}, \zeta^{\mathcal{T}+}] = \left[\zeta^{\mathcal{T}-} e^{-(\frac{x-\theta}{\delta})^2}, \zeta^{\mathcal{T}+} e^{-(\frac{x-\theta}{\delta})^2}\right]$, $[\zeta^{\mathcal{I}-}, \zeta^{\mathcal{I}+}] = \left[\zeta^{\mathcal{I}-} e^{-(\frac{x-\theta}{\delta})^2}, \zeta^{\mathcal{I}+} e^{-(\frac{x-\theta}{\delta})^2}\right]and[\zeta^{\mathcal{F}-}, \zeta^{\mathcal{F}+}] = \left[1 - (1 - \zeta^{\mathcal{F}-}) e^{-(\frac{x-\theta}{\delta})^2}, 1 - (1 - \zeta^{\mathcal{F}+}) e^{-(\frac{x-\theta}{\delta})^2}\right]$, $x \in X$, correspondingly, in which X refers to a non-empty set and $[\zeta^{\mathcal{T}-}, \zeta^{\mathcal{T}+}], [\zeta^{\mathcal{I}-}, \zeta^{\mathcal{I}+}], [\zeta^{\mathcal{F}-}, \zeta^{\mathcal{F}+}] \in Int([0,1])$ and $0 \le (\zeta^{\mathcal{T}+}(u))^2 + (\zeta^{\mathcal{I}+}(u))^2 + (\zeta^{\mathcal{F}+}(u))^2 \le 2$.

Assume $\hat{Z} = \langle (\theta, \delta); [\zeta^{\mathcal{T}-}, \zeta^{\mathcal{T}+}], [\zeta^{\mathcal{I}-}, \zeta^{\mathcal{I}+}], [\zeta^{\mathcal{F}-}, \zeta^{\mathcal{F}+}] \rangle$,$\hat{Z} = \langle (\theta_1, \delta_1); [\zeta_1^{\mathcal{T}-}, \zeta_1^{\mathcal{T}+}], [\zeta_1^{\mathcal{I}-}, \zeta_1^{\mathcal{I}+}], [\zeta_1^{\mathcal{F}-}, \zeta_1^{\mathcal{F}+}] \rangle$and $\hat{Z}_2 = \langle (\theta_2, \delta_2); [\zeta_2^{\mathcal{T}-}, \zeta_2^{\mathcal{T}+}], [\zeta_2^{\mathcal{I}-}, \zeta_2^{\mathcal{I}+}], [\zeta_2^{\mathcal{F}-}, \zeta_2^{\mathcal{F}+}] \rangle$ as three PNSNIVNs, and $r > 0$.

DOI: https://doi.org/10.54216/IJNS.250224
Received: February 23, 2024 Revised: May 12, 2024 Accepted: August 22, 2024

$$1.\ \hat{Z}_1 \oplus \hat{Z}_2 = \left[\begin{array}{c} (\theta_1+\theta_2, \delta_1+\delta_2); \\ \left[2r\sqrt{(\zeta_1^{\mathcal{T}-})^{2r}+(\zeta_2^{\mathcal{T}-})^{2r}-(\zeta_1^{\mathcal{T}-})^{2r}\cdot(\zeta_2^{\mathcal{T}-})^{2r}},\ 2r\sqrt{(\zeta_1^{\mathcal{T}+})^{2r}+(\zeta_2^{\mathcal{T}+})^{2r}-(\zeta_1^{\mathcal{T}+})^{2r}\cdot(\zeta_2^{\mathcal{T}\mp})^{2r}}\right] \\ r\sqrt{(\zeta_1^{\mathcal{J}-})^{r}+(\zeta_2^{\mathcal{J}-})^{r}-(\zeta_1^{\mathcal{J}-})^{r}\cdot(\zeta_2^{\mathcal{J}-})^{r}},\ r\sqrt{(\zeta_1^{\mathcal{J}+})^{r}+(\zeta_2^{\mathcal{J}+})^{r}-(\zeta_1^{\mathcal{J}+})^{r}\cdot(\zeta_2^{\mathcal{J}+})^{r}} \\ [\zeta_1^{\mathcal{F}-}\cdot\zeta_2^{\mathcal{F}-}, \zeta_1^{\mathcal{F}+}\cdot\zeta_2^{\mathcal{F}+}] \end{array}\right],$$

$$2.\ \hat{Z}_1 \otimes \hat{Z}_2 = \left[\begin{array}{c} (\theta_1+\theta_2, \delta_1+\delta_2);\ [\zeta_1^{\mathcal{T}-}\cdot\zeta_2^{\mathcal{T}-}, \zeta_1^{\mathcal{T}+}\cdot\zeta_2^{\mathcal{T}+}], \\ \left[r\sqrt{(\zeta_1^{\mathcal{J}-})^{2r}+(\zeta_2^{\mathcal{J}-})^{2r}-(\zeta_1^{\mathcal{J}-})^{2r}\cdot(\zeta_2^{\mathcal{J}-})^{2r}},\ r\sqrt{(\zeta_1^{\mathcal{J}+})^{2r}+(\zeta_2^{\mathcal{J}+})^{2r}-(\zeta_1^{\mathcal{J}+})^{2r}\cdot(\zeta_2^{\mathcal{J}+})^{2r}}\right] \\ 2r\sqrt{(\zeta_1^{\mathcal{F}-})^{r}+(\zeta_2^{\mathcal{F}-})^{r}-(\zeta_1^{\mathcal{F}-})^{r}\cdot(\zeta_2^{\mathcal{F}-})^{r}},\ 2r\sqrt{(\zeta_1^{\mathcal{F}+})^{r}+(\zeta_2^{\mathcal{F}+})^{r}-(\zeta_1^{\mathcal{F}+})^{r}\cdot(\zeta_2^{\mathcal{F}+})^{r}} \end{array}\right](\theta_1$$

$$3. r.\hat{Z} = \left[\begin{array}{c} (r.\theta, r.\delta); \\ \left[2r\sqrt{1-(1-(\zeta^{\mathcal{T}-})^{2r})^{r}},\ 2r\sqrt{1-(1-(\zeta^{\mathcal{T}+})^{2r})^{r}}\right], \\ [(\zeta^{\mathcal{J}-})^{r}, (\zeta^{\mathcal{J}+})^{r}], [(\zeta^{\mathcal{F}-})^{r}, (\zeta^{\mathcal{F}+})^{r}] \end{array}\right],$$

$$4.\ \hat{Z}^{r} = \left[\begin{array}{c} (\theta^{r}, \delta^{r}); [(\zeta^{\mathcal{T}-})^{r}, (\zeta^{\mathcal{T}+})^{r}], [(\zeta^{\mathcal{J}-})^{r}, (\zeta^{\mathcal{J}+})^{r}], \\ \left[2r\sqrt{1-(1-(\zeta^{\mathcal{F}-})^{2r})^{r}},\ 2r\sqrt{1-(1-(\zeta^{\mathcal{F}+})^{2r})^{r}}\right] \end{array}\right].$$

B. Stage II: GSO based Parameter Tuning

In the secondary stage, the hyperparameter tuning of the PNSNIVWA classifier endures by employing GSO. The GSO is a 2D workstation wherein every artificial agent, or glow, is transferring light and has its interpretation, called the local resolution area [18]. In order to find Luciferin's position, it must be needed to reflect its main values. The agent with high standards of intellect will be highly expected to fly in good locations (have a high-level main values). A neighbour with luciferin intensity larger than its magnitude with the local decision level can be distributed through the agent while it identifies a neighbor with luciferin intensity exceeding its degree. Based on the count of neighbors, there will be various local decision limitations. When the rise in threshold there will be some neighbors, and reduction in threshold while it has additional neighbors. In spite of which neighbor was chosen, the agent often modifies its way of movement. As luciferin ranges raise, a neighbor develops highly attractive. Likewise, majority of agents are positioned in numerous positions simultaneously. There are three primary stages to GSO such as the decision threshold stage, the motion stage, and luciferin update stage.

Luciferin updating stage: Luciferin is upgraded based on the gloss state values. Each glowworm starts with similar levels of luciferin, however, luciferin ranges differ with the activity level in the existing condition of glowworm, each have similar luciferin levels. The temperature and radiation ranges in a specific position finds the luciferin value. Every glowworm raises its luciferin level with its preceding level. Luminescence value should be subtracted from the preceding luminescence value for simulating the deterioration in the glow. The upgraded law of Luciferin values can be calculated as given below:

$$L_g(d+1) = (1-\rho)L_g(d) + \gamma J_g(d+1) \tag{1}$$

Luciferin range of a glowworm can be characterized by $L_g(d)$, ρ describes luciferin decline constant $0 < \rho < 1, \gamma$ denotes luciferin improvement constant, and J_g signifies a main operation in the position of i^{th} agents at t^{th} time.

Movement stage: This stage includes every individuals finding the movements of a neighbor with the large proportion of luciferin than itself by employing a probabilistic method. Neighbors who produce a brighter glow should be deliberated to attract glowworms. The possibility of every individual g moving to a neighbor h will be computed as denoted here,

$$P_{gh} = \frac{L_h(d) - L_g(d)}{\sum_{n \epsilon K_g(d)} L_n(d) - L_g(d)} \tag{2}$$

Now, $h \in K_g(d), K_g(d) = \{h; E_{g,h}(d) < P_E(d); L_g(d) < L_h(d)\}$ is a group of glowworm neighborhood g in time d. $E_{g,h}(d)$ signifies the ED among glowworms g and h at time d, and $\beta_E(d)$ indicates the neighborhood level related to g at time d. Consider glowworm g chooses a glowworm $h \in K_g(d)$ with $P_{gh}(d)$ specified by (2). Thus, glowworm movement will be defined as given below:

$$y_g(d+1) = y_g(d) + S(y_h\left(\frac{y_h(d) - y_g(d)}{\|y_h(d) - y_g(d)\|}\right) \tag{3}$$

DOI: https://doi.org/10.54216/IJNS.250224
Received: February 23, 2024 Revised: May 12, 2024 Accepted: August 22, 2024

Whereas S measns the step size, and $\|\|$ denotes the Euclidean norm operator.

Decision range updating: Each agent has been connected to a neighborhood where the radial level r_e^g is dynamic aspect $0 < r_e^g < r_S$. The sensor can be a radial range described as rS. This should be acceptable because there is no stable neighborhood level. While glowworms have been dependent only on local data in the movement, the count of peaks taken can differ based on the levels of the radial sensor. The agent whose sensor is proficient in hiding the whole search range can be moved to the global optimal. In this condition, there is no attention to the local optimum. Accordingly, determination of a neighborhood level to be appropriate for various processes landscapes will be complex without previous information on the main function (for example, peak number inter-peak distance and so on). In a common rule, main functions with decreased inter- peak distances higher than we have been chosen through those with decreased interpeak distances lesser than re. As a result, GSO identifies numerous peaks by employing adaptive neighborhood levels for the multimodal function landscape. While the resulting rule will be implemented, effectiveness will be drastically minimized:

$$r_{\mathrm{e}}^{g}(\mathrm{d}+1) = \min\left\{rS, \max\left\{0, r_{\mathrm{e}}^{g}(d) + \beta(kd - |Kg(d)|)\right\}\right\} \tag{4}$$

Eq. (4) can be represented as the constant parameter β and kd denotes number of neighbor variables. Fig. 2 depicts the flowchart of GSO.

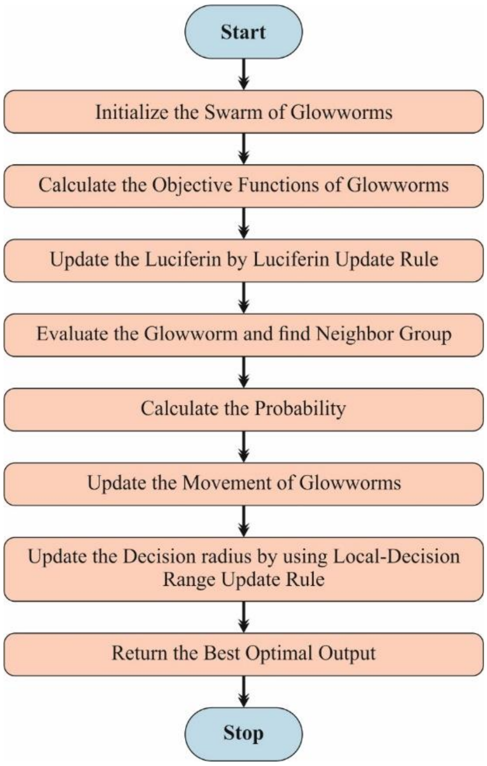

Figure 2. Flowchart of GSO

The GSO method is used to derive an FF to accomplish superior classifier outcomes. It defines a positive integer to characterize the enhanced performance of the solution candidate. Now, the reduction of the classifier error rate is regarded as an FF.

$$fitness(x_i) = ClassifierErrorRate(x_i) = \frac{No.of\ misclassified\ samples}{Total\ No.of\ samples} * 100 \tag{5}$$

4. Result Analysis and Discussion

This section studies the performance of the PNNIVWA-FRP method using a dataset [19] comprising 400 samples with two classes as depicted in Table 1.

DOI: https://doi.org/10.54216/IJNS.250224
Received: February 23, 2024 Revised: May 12, 2024 Accepted: August 22, 2024

Table 1: Details on Dataset

Class	No. of Instances
Financial Risk	200
Non Financial Risk	200
Total Instances	400

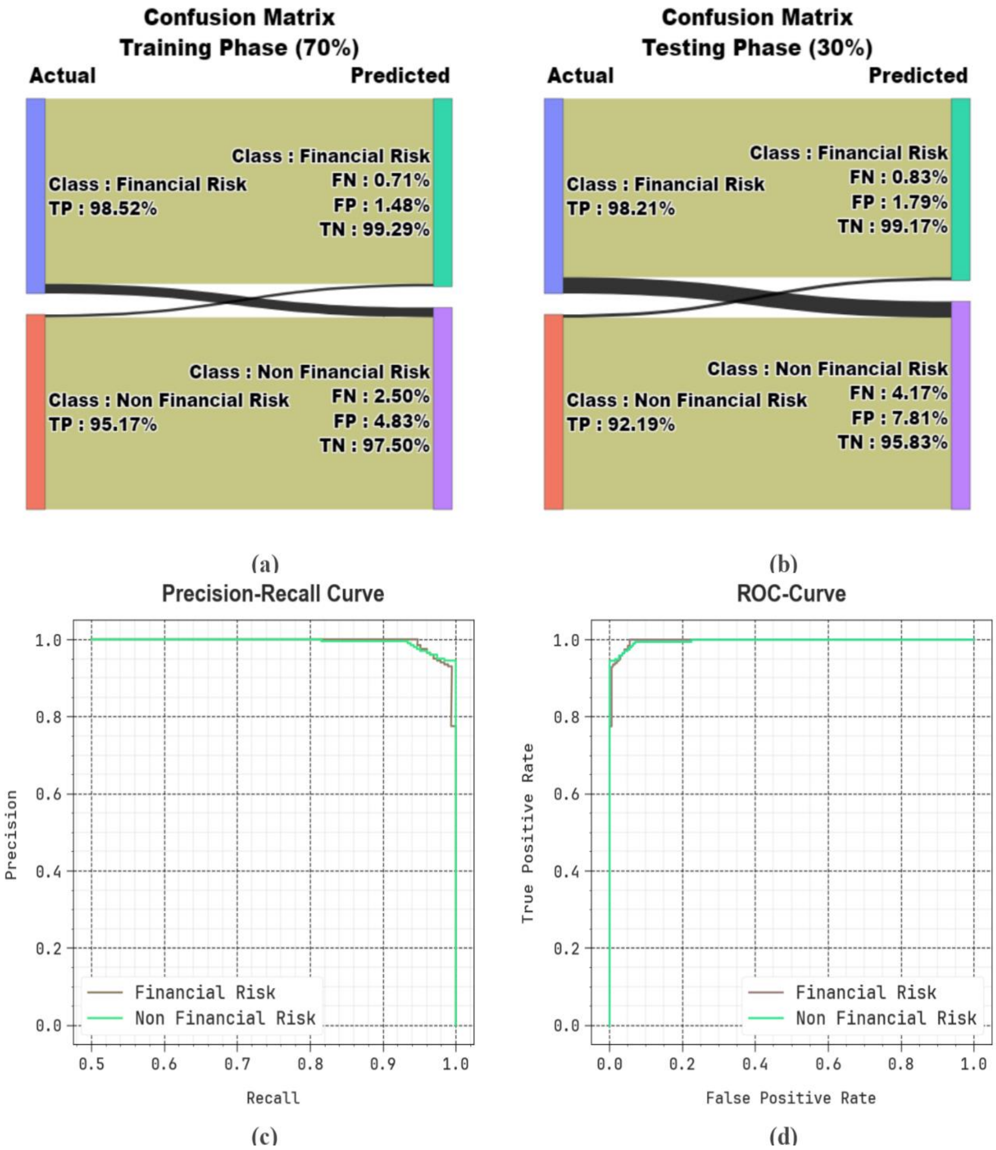

Figure 3. Classifier outcome of (a-b) 70% and 30% confusion matrices and (c-d) PR and ROC curves

Fig. 3 depicts the performance of the PNNIVWA-FRP technique in test dataset. Figs. 3a-3b shows the confusion matrices offered by the PNNIVWA-FRP method in 70% TRAP: 30% TESP. The outcome indicated that the PNNIVWA-FRP method has detected and classified all 2 classes accurately. Similarly, Fig. 3c certifies the PR examination of the DVNS-CKDDC technique. The outcome stated that the PNNIVWA-FRP model has increased maximum presentation of PR in every class. Finally, Fig. 3d displays the ROC investigation of the DVNS-CKDDC model. The outcome represented that the PNNIVWA-FRP approach has resulted in proficient results with maximum values of ROC on different classes.

DOI: https://doi.org/10.54216/IJNS.250224
Received: February 23, 2024 Revised: May 12, 2024 Accepted: August 22, 2024

In Table 2 and Fig. 4, the overall prediction outcomes of the PNNIVWA-FRP method with 70%TRAP and 30%TESP are depicted. The outcomes indicated that the PNNIVWA-FRP approach has properly detected two class labels. With 70%TRAP, the PNNIVWA-FRP system gains average $accu_y$ o 96.79%, $prec_n$ of 96.85%, $reca_l$ of 96.79%, $F1_{score}$ of 96.78%, and MCC of 93.63%. In addition, with 30%TESP, the PNNIVWA-FRP system gains average $accu_y$ o 95.00%, $prec_n$ of 95.20%, $reca_l$ of 95.00%, $F1_{score}$ of 94.99%, and MCC of 90.20%.

Table 2: Classifier outcome of PNNIVWA-FRP model under 70%TRAP and 30%TESP

Class	$Accu_y$	$Prec_n$	$Reca_l$	$F1_{Score}$	MCC
TRAP (70%)					
Financial Risk	95.00	98.52	95.00	96.73	93.63
Non-Financial Risk	98.57	95.17	98.57	96.84	93.63
Average	96.79	96.85	96.79	96.78	93.63
TESP (30%)					
Financial Risk	91.67	98.21	91.67	94.83	90.20
Non-Financial Risk	98.33	92.19	98.33	95.16	90.20
Average	95.00	95.20	95.00	94.99	90.20

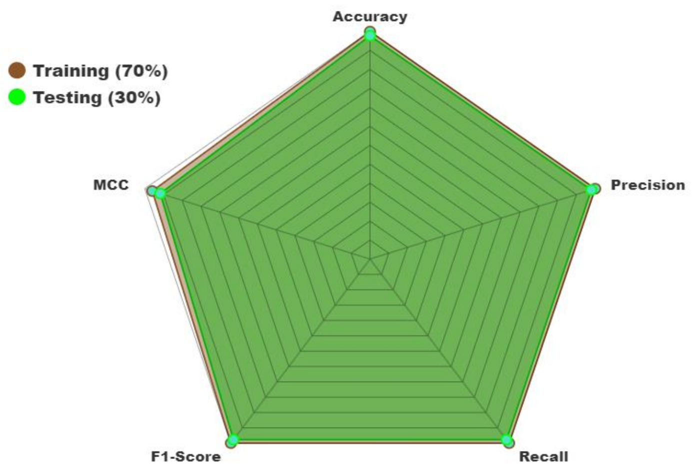

Figure 4. Average of PNNIVWA-FRP technique under 70%TRAP and 30%TESP

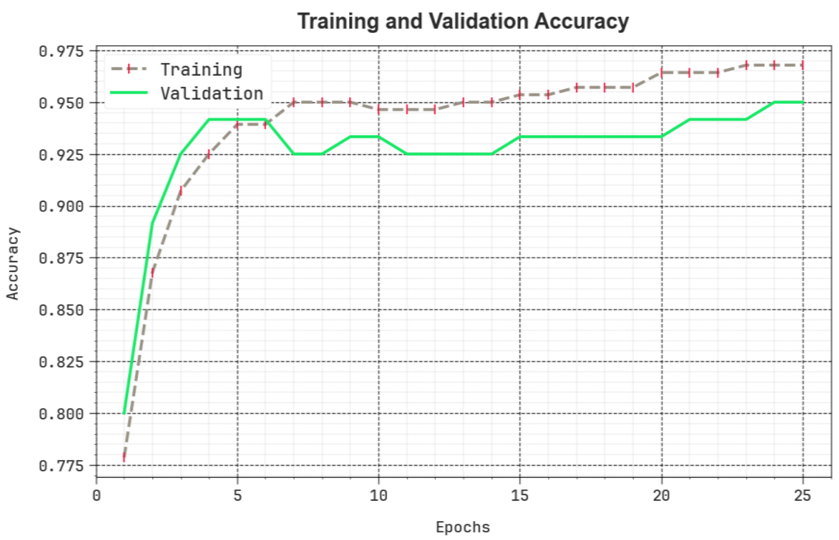

Figure 5. $Accu_y$ Curve of PNNIVWA-FRP technique

DOI: https://doi.org/10.54216/IJNS.250224
Received: February 23, 2024 Revised: May 12, 2024 Accepted: August 22, 2024

In Fig. 5, the training and validation accuracy outcomes of PNNIVWA-FRP technique are formed. The accuracy values are intended for 0-25 epochs. The result emphasized that the training and validation accuracy values show a rising tendency which informed the ability of the PNNIVWA-FRP technique with improved performance over many iterations. Furthermore, the training and validation accuracy remains nearer over the epochs, which describes least minimal overfitting and displays enhanced performance of the PNNIVWA-FRP model, assuring consistent prediction on hidden samples.

In Fig. 6, the training and validation loss graph of the PNNIVWA-FRP model is shown. The loss values are intended over a range of 0-25 epochs. It is explained that the training and validation accuracy values establish a declining tendency, which alerted the ability of the PNNIVWA-FRP technique to balance a trade-off amongst data fitting and generalization. The continual reduction in loss values also guarantees the amended performance of the PNNIVWA-FRP approach and tunes the prediction results over time.

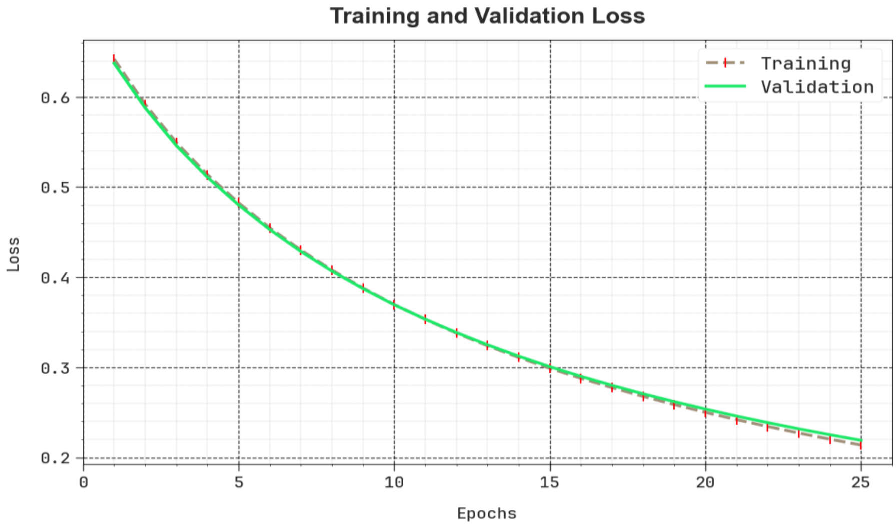

Figure 6. Loss curve of PNNIVWA-FRP model

Table 3 and Fig. 7 depict the comparison analysis of PNNIVWA-FRP methodology with other existing methods [20]. The table values stated that the PNNIVWA-FRP technique has exhibited optimum performances. Based on $accu_y$, the PNNIVWA-FRP system has gained higher $accu_y$ of 96.79% while the KNN, NB, DT, LR, and RF models have obtained lesser $accu_y$ of 94.06%, 91.04%, 94.48%, 90.32%, and 94.58%, correspondingly. Moreover, based on $prec_n$, the PNNIVWA-FRP method has got greater $prec_n$ of 96.85% while the KNN, NB, DT, LR, and RF models have obtained lesser $prec_n$ of 92.35%, 92.51%, 93.33%, 92.12%, and 91.33%, respectively. Eventually, based on $reca_l$, the PNNIVWA-FRP system has gained higher $reca_l$ of 96.79% while the KNN, NB, DT, LR, and RF models have obtained lesser $reca_l$ of 94.76%, 93.87%, 91.22%, 93.01%, and 93.29%, correspondingly.

Table 3: Comparative outcome of PNNIVWA-FRP method with other techniques

Techniques	$Accu_y$	$Prec_n$	$Reca_l$	$F1_{Score}$
KNN Algorithm	94.06	92.35	94.76	90.92
Naïve Bayes	91.04	92.51	93.87	95.11
Decision Tree	94.48	93.33	91.22	94.61
Logistic Regression	90.32	92.12	93.01	93.72
Random Forest	94.58	91.33	93.29	90.76
PNNIVWA-FRP	96.79	96.85	96.79	96.78

DOI: https://doi.org/10.54216/IJNS.250224
Received: February 23, 2024 Revised: May 12, 2024 Accepted: August 22, 2024

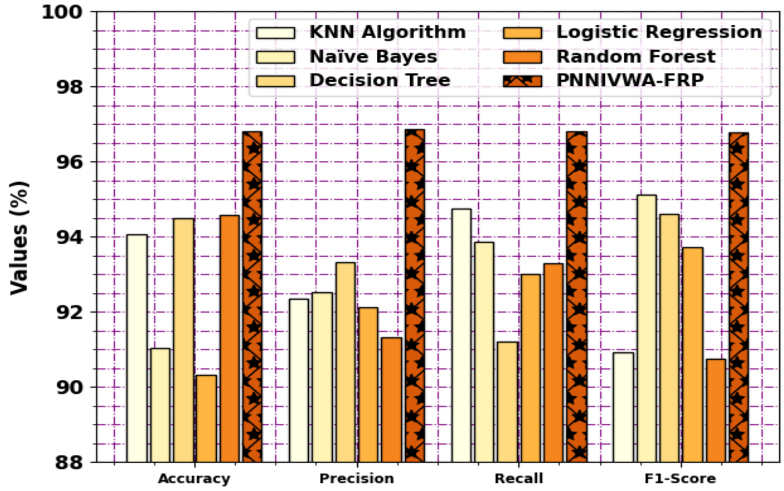

Figure 7. Comparative outcome of PNNIVWA-FRP method with other techniques

5. Conclusion

In this study, we design a new PNNIVWA-FRP method using sustainable development. The main purpose of the PNNIVWA-FRP algorithm is to have two different stages of processes. Initially, the financial data can be classified by the PNSNIVWA technique. This method is used for its highest proficiency in managing imprecision and uncertainty in financial data, containing incomplete and ambiguous data. Second, the classified parameter is fine-tuned by means of GSO technique. Based on the luminescent communication of glowworms, GSO is proficient at navigating multidimensional, complex search spaces for identifying better solutions. The empirical findings on benchmark dataset validate the efficiency of the PNNIVWA-FRP algorithm, showcasing significant development in prediction results than classical approaches.

Funding: “The authors extend their appreciation to the Deanship of Research and Graduate Studies at King Khalid University for funding this work through Large Research Project under grant number RGP2/353/45”

Conflicts of Interest: “The authors declare no conflict of interest.”

References

[1] Parimala, M., Karthika, M. and Smarandache, F., 2020. A review of fuzzy soft topological spaces, intuitionistic fuzzy soft topological spaces and neutrosophic soft topological spaces. International Journal of Neutrosophic Science, Vol. 10, No. 2, 2020, PP. 96-104.

[2] Ashraf, S. and Abdullah, S., 2020. Decision support modeling for agriculture land selection based on sine trigonometric single valued neutrosophic information. International Journal of Neutrosophic Science (IJNS), 9(2), pp.60-73.

[3] Ashraf, S. and Abdullah, S., 2020. Decision support modeling for agriculture land selection based on sine trigonometric single valued neutrosophic information. International Journal of Neutrosophic Science (IJNS), 9(2), pp.60-73.

[4] Al-Hamido, R.K., Salha, L. and Gharibah, T., 2020. Pre Separation Axioms In Neutrosophic Crisp Topological Spaces. International Journal of Neutrosophic Science, 8(2), pp.72-79.

[5] Salama, A.A., Henawy, M.B. and Alhabib, R., 2020. Online Analytical Processing Operations via Neutrosophic Systems. International Journal of Neutrosophic Science, 8(2), pp.87-109.

[6] Liu, Y., Liu, L. and Ren, G., 2019. Financing Risk Prediction of China's Listed Company based on GA-SVR Model. Journal of Beijing Institute of Technology (Social Sciences Edition), (4), pp.73-81.

[7] Valaskova, K., Kliestik, T., Svabova, L. and Adamko, P., 2018. Financial risk measurement and prediction modelling for sustainable development of business entities using regression analysis. Sustainability, 10(7), p.2144.

[8] Peng, X. and Huang, H., 2020. Fuzzy decision making method based on CoCoSo with critic for financial risk evaluation. Technological and Economic Development of Economy, 26(4), pp.695-724.

DOI: https://doi.org/10.54216/IJNS.250224
Received: February 23, 2024 Revised: May 12, 2024 Accepted: August 22, 2024

[9] Ashraf, S., GS Félix, E. and Serrasqueiro, Z., 2019. Do traditional financial distress prediction models predict the early warning signs of financial distress?, Journal of Risk and Financial Management, 12(2), p.55.

[10] Li, J., Yang, L., Smyth, B. and Dong, R., 2020, October. Maec: A multimodal aligned earnings conference call dataset for financial risk prediction. In Proceedings of the 29th ACM International Conference on Information & Knowledge Management (pp. 3063-3070).

[11] Hou, L., Lu, K. and Bi, G., 2024. Predicting the credit risk of small and medium-sized enterprises in supply chain finance using machine learning algorithms. Managerial and Decision Economics, 45(4), pp.2393-2414.

[12] Lei, Y., Qiaoming, H. and Tong, Z., 2023. Research on supply chain financial risk prevention based on machine learning. Computational Intelligence and Neuroscience, 2023(1), p.6531154.

[13] Gu, Z., Lv, J., Wu, B., Hu, Z. and Yu, X., 2024. Credit risk assessment of small and micro enterprise based on machine learning. Heliyon, 10(5).

[14] Shen, H., 2023. Assessment of financial risk pre-alarm mechanism based on financial ecosystem using BPNN and genetic algorithm. Soft Computing, 27(24), pp.19265-19279.

[15] Zhang, J., 2024. Impact of an improved random forest-based financial management model on the effectiveness of corporate sustainability decisions. Systems and Soft Computing, 6, p.200102.

[16] Ma, Z., Wang, X. and Hao, Y., 2023. Development and application of a hybrid forecasting framework based on improved extreme learning machine for enterprise financing risk. Expert Systems with Applications, 215, p.119373.

[17] Palanikumar, M., Arulmozhi, K. and Jana, C., 2022. Multiple attribute decision-making approach for Pythagorean neutrosophic normal interval-valued fuzzy aggregation operators. Computational and Applied Mathematics, 41(3), p.90.

[18] Chavan, R. and Pete, D., 2024. Automatic multi-disease classification on retinal images using multilevel glowworm swarm convolutional neural network. Journal of Engineering and Applied Science, 71(1), p.26.

[19] https://www.kaggle.com/datasets/manukulamkombil/machinehack-financial-risk-prediction?select=Train.csv

[20] Dong, H., Liu, R. and Tham, A.W., 2024. Accuracy Comparison between Five Machine Learning Algorithms for Financial Risk Evaluation. Journal of Risk and Financial Management, 17(2), p.50.

DOI: https://doi.org/10.54216/IJNS.250224
Received: February 23, 2024 Revised: May 12, 2024 Accepted: August 22, 2024